Ti-2007 Science and Technology, edited by M. Ninomi, S. Akiyama, M. Ikeda, M. Hagiwara, K. Maruyama
The Japan Institute of Metals (2007)

Optimization of Hot Workability and Control of Microstructure During Hot Deformation of Ti53311S Alloys

Ruining Wang[1,2], Zhengping Xi[2], Yongqing Zhao[2], Yunlian Qi[2], Yu Du[2], Xiaonan Du[2]

[1]School of Materials Science and Engineering, Xi'an University of Architecture and Technology, Xi'an 710055, China

[2]Northwest Institute for Nonferrous Metal Research (NIN), Xi'an 710016, China

The hot deformation characteristics of Ti53311S alloys have been studied in the temperature from 880°C to 1080°C and in the strain rate range from $10^{-3}s^{-1}$ to $10s^{-1}$ by constructing power dissipation maps which describe the variation of the efficiency of power dissipation with temperature and strain rate. The processing maps showed domains at some combinations of temperature and strain rates and these domains have been correlated with specific microstructure processes occurring during hot deformation by metallographic investigations and kinetic analysis. Various deformation mechanisms like dynamic recrystallization (DRX), dynamic recover have been identified in the alloys studied depending on the strain rate and temperature. The flow instability during hot deformation has also been investigated and the deformation conditions that favor DRX process is recommended for hot working.

Keyword: Ti53311S alloys, hot deformation, processing maps, microstructure, dynamic recrystalization, dynamic recovery

1. Introduction

Ti53311S is a near alpha titanium alloy, which service temperature can reach to 550°C, mostly used for aerospace, possessing an attractive combination of properties, such as thermal stability, high temperature instantaneous intensity and creep resistance. With the development of the technology of precise formation, it is necessary to control the microstructure of materials during deformation. Therefore, it is important to understand the relationships among processing variables, microstructures and deformation behavior. The compressive characteristics, processing maps and microstructural variation of Ti53311S alloy over a range of deformation temperatures and strain rates were studied in this paper. The processing maps have been reported in many papers[1-6], which are being used for optimizing the hot working parameters and controlling the microstructure of hot worked material.

2. Experimental Material and Procedures

The experimental material was supplied by NIN, which is a bar of 14.5 mm in diameter. Its nominal beta transus is 1010°C. The microstructure of Ti53311S alloy bar is shown in **Figure 1**.

Figure 1. Optical micrograph of Ti53311S alloy before deformation

Hot compressive deformation behavior of Ti53311S alloy at elevated temperatures was studied on Gleeble 1500 thermal simulator using cylindrical specimens (8mm in diameter and 12mm in height). The specimens were directly electrified to heat and the temperature was controlled with a thermocouple spot welded on the specimen surface. In the present investigation, the compressive tests were performed at deformation temperatures ranging from 880 to 1080°C and at strain rates from $10^{-3}s^{-1}$ to $10s^{-1}$. The specimens were held for 5min at the deformation temperature before the commencement of deformation to ensure homogeneous temperature fields. After completion of the required deformation, the

specimens were quenched by water quickly to retain the deformed microstructures for microstructural investigation. The compressibility is 60%. In order to reduce frictions, two ends of the specimen and the indenter of Gleeble 1500 thermal simulator were coated with graphit lubricant. The microstructure of Ti53311S alloy was observed and analyzed using Olympus optical microscope.

3. Results and Discussions

3.1 Flow Stress Behavior

The shapes of the flow curves exhibited by the material at different temperatures and strain rates of testing are shown in **Figure 2**. Flow stress data at different temperatures, strain rates and strains are given in **Table 1**.

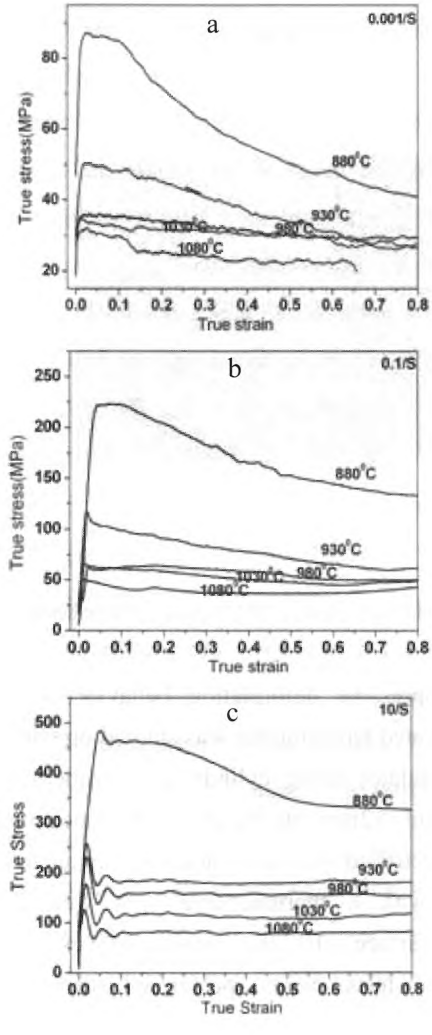

Figure 2. Trues stress-true strain at different strain rate (a)0.001s^{-1} (b)0.1s^{-1} (c) 10s^{-1}

In **Figure 2a**. the flow stress decreases quickly with the increasing of strain at 880°C and 1030°C, which are indicative of steady state flow behavior. The softening features of curves are similar in **Figure 2b**, and the continuous flow softening was observed after a peak stress at strain rate of 0.1s^{-1} and different temperatures. In **Figure 2c**, at strain rates of 10s^{-1} and all temperatures of testing, a discontinuous softening in the flow stress with strain as recorded. These observations indicate the possibility of hot shearing, grain growth coarsing or globurizing. It can be seen that this material is sensitive to temperature and strain rate, especially strain rate.

Table 1. Flow stress values of Ti53311S alloy (MPa) at different temperature and strain rates for various strains

Strain (ε)	Strain rate (s^{-1})	Temperature(°C) 880	930	980	1030	1080
0.2	0.001	64.4	45.3	30.7	31.8	25.4
	0.01	115.6	66.2	44.7	40.2	34.0
	0.1	204.4	91.2	66.1	58.6	40.9
	1	343.5	182.3	117.2	77.6	60.7
	10	457.6	185.3	160.5	118.3	82.8
0.3	0.001	55.7	40.88	28.2	33.1	24.1
	0.01	104.3	58.0	41.7	37.4	31.9
	0.1	182.9	83.7	62.6	54.3	37.4
	1	322.8	178.1	116.3	78.0	61.9
	10	386.7	179.0	159.8	116.5	83.8
0.4	0.001	49.1	36.9	26.4	30.1	23.6
	0.01	96.0	53.1	39.1	34.8	30.6
	0.1	165.4	78.0	60.9	50.21	36.9
	1	286.4	176.6	115.4	76.1	60.8
	10	386.7	179.0	157.3	110.6	80.7
0.5	0.001	43.1	33.8	25.1	30.3	22.5
	0.01	86.9	49.0	35.9	32.5	29.6
	0.1	152.9	71.1	56.3	47.8	36.5
	1	286.4	176.1	112.3	76.4	59.9
	10	347.7	179.6	156.9	108.8	78.8
0.6	0.001	38.7	31.2	21.8	28.5	21.4
	0.01	80.7	44.9	34.2	30.4	28.8
	0.1	144.4	65.8	52.6	45.4	37.2
	1	272.8	166.5	109.7	75.5	60.7
	10	333.1	184.4	155.7	107.8	80.4

3.2 Processing Map

The processing map has been adopted in this study to represent and analyze the constitutive behavior of Ti53311S alloy during hot deformation. Depicted in a frame of temperature and strain rate, a power dissipation map represent the pattern in which the input power ($\sigma\ \dot{\varepsilon}$) is dissipated by the material through microstructural changes rather than heat. Here σ is strain strength, and $\dot{\varepsilon}$ is strain rate. The rate of this change compared to an ideal liner dissipater is given by the dimensionless parameter called

the efficiency of power dissipation[7]:

$$\eta = \frac{2m}{m+1} \quad (1)$$

Where m is strain rate sensitivity of flow stress. Over this frame, an instability map developed using the continuum instability criterion[8] given by

$$\zeta(\dot{\varepsilon}) = \frac{\partial \ln[m/(m+1)]}{\partial \ln \dot{\varepsilon}} + m < 0 \quad (2)$$

Then a power dissipation map and an instability map are superimposed to obtain a processing map. Flow instabilities are predicted to occur when the dimensionless instability parameter ξ becomes negative[8]. The procedure adopted for developing a processing map using the flow stress data given in Table 1 is briefly described. Processing map developed for Ti53311S at a strain of 0.6 is shown in **Figure 3** in which contour numbers represent percent η and shade area correspond to negative ξ regime. Maps at strains less than 0.6 exhibited essentially similar features.

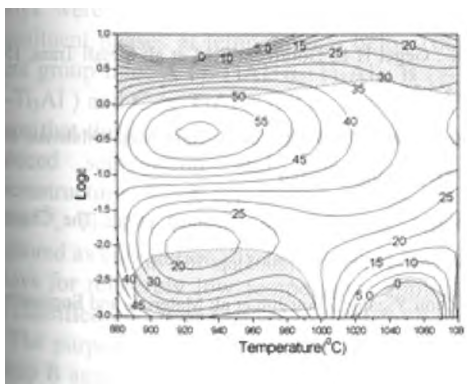

Figure 3. Processing maps for Ti53311S alloy obtained at strain of 0.6

The map exhibits a larger regime of flow instability and two domains where the efficiency of power dissipation reaches a local maximum. The characteristics of these domains are described below.

Domain 1 occurs in the temperature from 900 to 960°C and strain rate from 0.1 to $1s^{-1}$, and has a peak efficiency higher than 55% at 930°C and $0.32s^{-1}$.

Domain 2 occurs in the temperature from 880 to 900°C and strain rate $0.001s^{-1}$, and has a peak efficiency higher than 45% at 880°C and $0.001s^{-1}$.

The regime of flow instability occurs in the strain rate higher than $1s^{-1}$ and lower than $0.01s^{-1}$, temperature from 880 to 1080°C. In view of these changes, it may be possible that different microstructural mechanisms with similar dissipation characteristic are occurring in this domain and hence the interpretation of this domain will require detailed microstructural observations.

3.3 Microstructural Mechanisms

Microstructures of specimens deformed at 930°C and different strain rate in domain 1 and domain 2 are shown in **Figure 4a-d.** In **Figure 4**, majority of the alpha matrix are observed in the compression specimens and the alpha grains are thinner. The recrystal grain is not discovered in the microstructure, then the relaxation of stress accumulation may occur by dynamic recover. Micrographs of specimen deformed at 930°C and $1s^{-1}$ is shown in **Figure 4c**, which exhibit globularization of colony structure. These micrographs clearly reveal that the curving α grain produced after globularization. Considering the higher energy needed during globularization, such high efficiency of power dissipation of about 55% in this domain could be attributed to globularization.

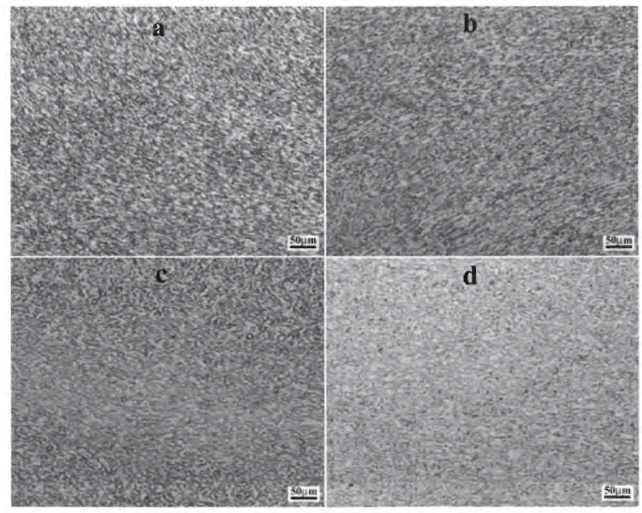

Figure 4. Microstructures of Ti53311S alloy compressed with different strain rate and temperature (a) 930°C $0.1s^{-1}$ arc; (b) 930°C $1s^{-1}$ arc; (c) 930°C,$0.1s^{-1}$ middle (d) 880°C, $0.001s^{-1}$ arc

Microstructural observations showed that the pile-up of dislocation at the plate alpha grain boundary and dislocation tangle, as shown in **Figure 5a-b**. Because dynamic recrystallization relaxes the stress accumulation with much faster rates comparing with recovery to mitigate the aggregation of dislocation. We can deduce that the deformation mechanism is dynamic recover but not recrystallization in domain 1 due to the large dislocations observed in **Figure 5**. Domain 2 was characterized by dynamic recover, only elongated alpha grains, no recrystallized grains could be observed in this region, as shown in **Figure 4d**, which was similar to the original structure.

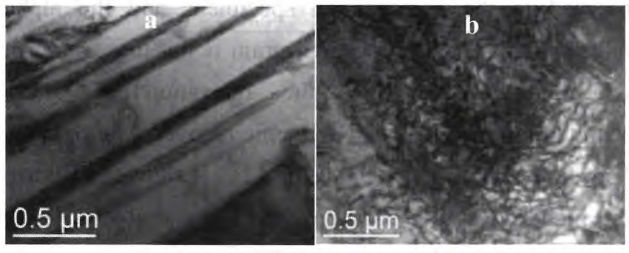

Figure 5. TEM microstructure of Ti53311S alloy compressed at 930°C and $0.1s^{-1}$

In **Figure 6**., microstructural observations showed that the coarsing grain which occurs in the temperatures of 1030°C and strain rate $0.001s^{-1}$ and $10s^{-1}$. In this region, the processing map displayed a broad unstable flow with a low efficiency of power dissipation.

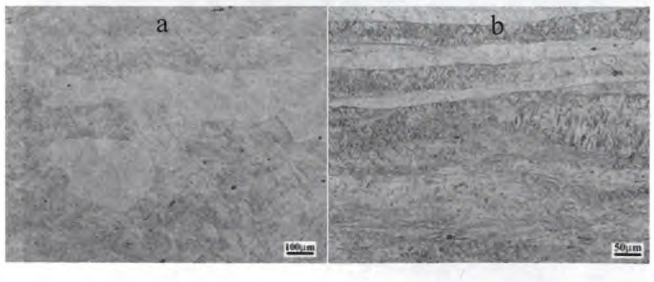

Figure 6. Microstructure of Ti53311S alloy compressed with different strain rate and at 1030°C (a) $0.001s^{-1}$; (b) $10s^{-1}$

Such a microstructure may be attributed to the adiabatic conditions created during deformation and low thermal conductivity of Ti53311S alloy , and the tendency of which will be greater at higher strain rate or lower temperature, although apparent shear cracking was not observed in the deformed specimens. These instability regimes identified above must be avoided during hot working of Ti53311S alloy in order to obtain a defect-free microstructure.

4 Conclusions

Ti53311S alloy is sensitive to temperature and strain rate, especially strain rate; The deformation mechanism of this material is dynamic recover and globularization in the studied range of this paper. The range of work is narrow, and the optimal hot working condition is at the temperature below transformation point and strain rate higher than $0.01s^{-1}$ and lower than $1s^{-1}$.

Acknowledgment

The authors wish to thank the support of National Important Natural Science Foundation of China.(50434030)

REFERENCE

1) Bozzini B, Cerri E: Mater Sci Eng A. **A328** (2002)pp. 344-347.

2) Rao K P, Doraivelu S M, Prasad Y V R K et al: Metall Trans. **14A** (1983) pp. 1671.

3) Prasad Y V R K, Gegel H L, Doraivelu S M et al: Metall Trans, **15A** (1984) pp.1883.

4) Zhou Jun, Zeng Weidong, Shu Ying et al: Rare Metal Materials and Engineering. **35** (2006) pp.265-269.

5) Huang Guangsheng, Wang Lingyun, Chenhua et al: The Chinese Journal of Nonferrous Metal. **15** (2005) pp. 763-767.

6) Zeng Weidong, Zhou Yigang, Zhou Jun et al: Materials and Engineering. **35** (2006) pp.673~677.

7) Prasad Y V R K et al: Indian J Tech. **28** (1990) pp.435.

8) Prasad Y V R K, S. Sasidhara: *Hot working Guide: A compendium of processing maps*,(ASM International, Materials Park, OH, (1997)) pp 101-102.

9) S.M.L. Sastry, R.J.Lederich, T.L.Mackay, W.R.Kerr: Metals. **35** (1983) pp. 48-53.